Received: 24 May 2019 | Revised: 7 June 2019 | Accepted: 19 June 2019

DOI: 10.1111/jocd.13083

ORIGINAL CONTRIBUTION

JCD Journal of Cosmetic Dermatology WILEY

# Facial rejuvenation using Er:YAG laser equipped with a spatially modulated ablation module: A clinical, ultrasound, and histological evaluation

Natalia V. Volkova PhD, MD[1] | Irene E. Valamina PhD[2] | D. V. Shvidun MD[3] | A. S. Rebrieva MD[3] | Neil S. Sadick MD[4]

[1]Department of Aesthetic Medicine, Ural State Medical University, Yekaterinburg, Russia

[2]Department of Pathological Anatomy, Histological laboratory of TsNIL UGMU, Ekaterinburg, Russia

[3]Linline" Clinic Chain, Minsk, Belarus

[4]Weill Cornell Medical College, Sadick Dermatology, New York, NY, USA

**Correspondence**
Neil S. Sadick, Weill Cornell Medical College, Sadick Dermatology, 911 Park Avenue, New York, NY 10075.
Email: nssderm@sadickdermatology.com

## Abstract

**Background:** A plethora of noninvasive approaches has been developed in recent years for facial rejuvenation. Energy-based devices have been one of the most popular treatments for reversing and preventing signs of facial aging such as fine lines, wrinkles, ptosis, and photoaging.

**Aims:** A new technology (RecoSMA) for skin rejuvenation based on acoustic-interference method using Er:YAG laser (2936 nm) equipped with a special module that targets both the dermis and the superficial musculoaponeurotic system (SMAS) was recently demonstrated to be safe and effective in facial rejuvenation.

**Patient/Methods:** In this follow-up prospective study, the clinical effects of recoSMA treatment on skin structures and SMAS were evaluated with ultrasound and histological analysis, at 30 and 90 days posttreatment.

**Results:** Treatment with recoSMA was shown to result in a significant increase in thickness of the epidermis, dermis, and SMAS layer, while levels of collagen I, III, and IV were shown to be elevated at 90 days posttreatment.

**Conclusion:** Collectively, data show that treatment with recoSMA laser has a profound biological effect in stimulating and reconstructing the elastin/collagen framework necessary for preventing facial aging.

KEYWORDS
Er:YAG laser, facial rejuvenation, histology, superficial musculoaponeurotic system, ultrasound

## 1 | INTRODUCTION

The pathophysiology underlying facial aging is complex and influenced by intrinsic (genetics) and extrinsic (lifestyle, UV exposure) factors. Manifestations of aging, such as wrinkles, laxity, and fine lines first show on the face and neck, due to the fact that it is continuously exposed to the environment and because of the inherent nature of facial skin and relevant structures. The biological effects of facial aging have been extensively characterized and include depletion of superficial and deep adipose compartments, gradual loss of bone, thinning and disorganization of the collagen/elastin content of the epidermis and dermis, and loosening of the superficial musculoaponeurotic system (SMAS).[1,2] Detailed analysis of fibroblast function and collagen-elastin framework in aged skin has revealed that the SMAS ligaments stretch, lengthen, and change their direction from horizontal to vertical.[3] This directional change results in loosening of the SMAS framework and under the action of gravity, it is shifted down.[4,5]

In the past few years there has been a surge of aesthetic interventions that aim to reverse and prevent the signs of aging. While

  

decades ago surgical approaches such as rhytidectomy and facelift were the main methodologies applied to patients seeking anti-aging treatments, today due to scientific and technological innovations there is a gamut of noninvasive choices available.[6] From injectable fillers, neurotoxins, to new-generation chemical peels and cutting-edge energy-based devices, facial rejuvenation has become prevalent and adopted by men and women of all ages, ethnicities, and cultures.[7]

The most effective treatments for facial rejuvenation are those that require minimal downtime, have a high-safety profile and where results can be observed within months of the procedure. Since different approaches typically target one indication or facial structure, a combination of treatments is often required to deliver optimal clinical outcomes. With regard to energy-based devices such as radiofrequency, ultrasound and laser modalities, these are primarily based on a thermal mechanism of action.[8] To this end, existing devices such as ablative fractional lasers require extensive downtime, or alternatively compromise efficacy and outcomes in order to minimize risk and severity of adverse effects.

We recently described a novel laser for skin rejuvenation, Recovery Spatially Modulated Ablation (RecoSMA), that combines an Er:YAG (2936 nm) laser with a spatial modulated ablation (SMA) module that delivers acoustic wave energy.[9] By delivering laser energy, this device creates zone of microablation in the upper epidermis while with the acoustic-interference mediated by the SMA module, acoustic waves penetrate the skin depth to 6 mm reaching the dermis/SMAS interface, stimulating neocollagenesis. Unique features of this technology lie in the nonthermal mechanism of action, which makes for a comfortable treatment for patients and keeps the downtime minimal.[10-12] Moreover, since the energy is delivered to all the skin layers from the epidermis, to the dermis and SMAS, the treatment is considered comprehensive compared to lasers targeting only one facial structure.[10-12] Once neocollagenesis and the "lifting" process are triggered, rehabilitation and clinical improvement continues for 3 months. To date, recoSMA has been used for a wide range of indications, such as photoaging, laxity, ptosis, acne scars, enlarged pore, and striae distensae.[13]

In a previous prospective study, we demonstrated the safety and efficacy of recoSMA for facial rejuvenation in a cohort of patients. The objective of this follow-up prospective study is to thoroughly assess via ultrasound and histological analysis, the biological effects of recoSMA on the epidermis, dermis, and SMAS at 30 and 90 days after the treatment.

## 2 | MATERIALS AND METHODS

### 2.1 | Patients

This was a prospective study conducted in accordance with the principles of the Declaration of Helsinki, current GCP guidelines, and IRB approval. A total of 71 patients (68 women, three men) 34 to 72 years old were enrolled in the study. All patients provided written, informed consent. Exclusion criteria included the following: pregnancy, breastfeeding, internal chronic disease, infectious disease, active skin disease (such as infection, psoriasis, eczema, and various dermatitis), autoimmune disease, or skin cancer. If the subjects received any other investigational treatment or had participated in another clinical study within 6 months prior to study enrollment, they were excluded.

### 2.2 | Laser treatment

All patients received one treatment with the Erbium-YAG Laser equipped with the 5 mm SMA module (LINLINE Medical Systems, Minsk, Belarus). Before the treatment, the patient's skin was cleaned and dried. The procedure was done without anesthesia. The treatment parameters were 2.21 J/cm$^2$ and 3 Hz. The target areas spanned from the hairline to the chin. Pulses were applied using scan patterns such as "olympic rings."

For antiviral prevention, all patients used systemic acyclovir 1000 mg/d the day of treatment and two days after laser therapy. During the recovery period, patients were instructed to wipe the skin with tissue and 0.05% chlorhexidin the digluconate solution and apply 5% dexpanthenol cream on the skin 2-3 times per day.

### 2.3 | Photography

Standardized clinical photography was conducted at baseline, 30, and 90 days after treatment. All patients were photographed from five sides: full face, right and left side views, right and left three quarter views.

### 2.4 | Ultrasound analysis

Ultrasound skin examination was conducted on all patients on the SkinScanner DUB CUTIS 22 MHz. The measurement point was 1.5 cm from the lateral eye cantus. The following parameters were assessed: thickness of the epidermis, dermis, hypodermis, SMAS, the surface area of serrated hypodermis-dermis junction and the density of the dermis, and SMAS.

### 2.5 | Histological analysis

Histological examination was done using punch biopsy (Dermapunch 2 mm) prior to treatment (baseline biopsy) and 3 months after the procedure in two female patients (46 and 52 y.o.). Lidocaine (1% solution) was applied to the skin prior to punch biopsy. The biopsy sites were 0.4 cm above the edge of the mandible, in the projection of the masticatory muscle. Specimens were preserved in 10% neutral formalin, dehydrated in a series of alcohols and embedded in paraffin observing the orientation of the sections. Histological sections were obtained on the NM-450 MICROM microtome. After microtomy, histological sections were stained (section thickness 5-7 μm) with hematoxylin and eosin, combined Weigert's elastic stain, and van Gieson's stain. Immunohistochemical study was performed on paraffin sections with an immunoperoxidase method using antibodies to collagen I (Rabbit Polyclonal), III (Rabbit Polyclonal), and

IV (CIV22) types. Light microscopy survey of obtained histological specimens was done using the Olympus CX41 light microscope with ×50, 100, 200, 400, 600 magnification. The photomicrography was taken using a camera to detect the morphological changes.

### 2.6 | Statistical analysis

Ordinal variables were analyzed using Wilcoxon test for paired samples. For ratio scaled variables normal distribution was verified by Kolmogorov-Smirnoff test and then analyzed using Student's *t* test for paired variables or Wilcoxon test. All statistical tests were two-sided and tested in conjunction with a 0.05 nominal significance level. Analyses were carried out using an IBM SPSS Statistics 22.0 system.

## 3 | RESULTS

### 3.1 | Clinical efficacy

All 71 patients completed the study. Patients were seen for clinical photography and ultrasound evaluation at 30 and 90 days after a single laser treatment. Comparison of baseline photographs with those at the 30 and 90 day follow-up revealed time-dependent gradual improvement of skin structure, color, decrease of wrinkle depth, and lifting of soft tissues. Maximal improvement was demonstrated at the 90-day follow-up visit (Figures 1, 2). Patient satisfaction was high, and the procedure was well tolerated. The recovery period did not exceed 7 days for any of the patients and no adverse effects were observed.

### 3.2 | Utrasound analysis results

At baseline, the mean epidermal thickness was 132.21 mm, while at 30 and 90 days posttreatment it was 138.41 mm and 134.87 mm, respectively (Table 1). The mean dermal thickness was 1324.64 mm at baseline, 1422.09 mm after 30 days, and 1489.58 mm at 90 days posttreatment. Thus, there was a 7.36% increase of the dermal thickness at 30 days, and a 12.45% increase at 90 days which was statistically significant. At baseline, mean dermal density was −12.64, while at 30 and 90 days posttreatment it was −13.45 and −16.08, respectively, resulting in a 27.22% statistically significant increase in dermal density. The hypodermal thickness increased from 434.81 mm at baseline to 473.75 mm and 448.38 mm at 30 and 90 days posttreatment but the increase was not statistically significant. The SMAS thickness was measured at 180.38 mm at baseline and increased to 209.01 mm and 239.87 mm at the 30- and 90-day follow-up time points. Both the 30- and 90-day increase (15.94% and 32.98%, respectively) in SMAS thickness was statistically significant (Table 1). Mean SMAS density was −18.93 at baseline, −20.84 after 30 days, and −27.39 90 days posttreatment (Table 1). Only the increase in SMAS density at 90 days posttreatment (44.7%) was shown to be statistically significant.

The evenness of the boundary between the dermis and hypodermis was also assessed at baseline, 30, and 90 days posttreatment and analysis of ultrasound data revealed a statistically significant increase in evenness of the boundary from 50.7% at baseline to 71.8% and 77.6% at 30 and 90-days posttreatment, respectively (Figure 3). The cohesivity of the SMAS layer was also analyzed via ultrasound and was shown to increase from 50.7% at baseline, to 63.4% and 78.9% at 30 and 90 days, respectively. The increase in SMAS cohesivity was statistically significant at 90 days posttreatment. The gradual increase in dermal SMAS thickness and density is shown in Figure 4.

### 3.3 | Histological analysis results

Histological analysis revealed that at baseline, the epidermis was unevenly thinned, the dermal-epidermal junction was violated, while the epidermal basal membrane was thickened, and defibrated (Figure 5A). At the 90-day follow-up, histological analysis demonstrated an increase in epidermal thickness, and epidermal ridges at the dermal-epidermal junction indicative of tissue growth (Figure 5B). In the dermis, elastic fibers were found to be fragmented, with areas of elastic fiber


**FIGURE 1** Patient 55 y.o. before (A) and 3 mo after treatment (B). Improvement in facial color, skin tone, shallower wrinkles, lifting effect in the middle and lower thirds of the face, including shallower nasolabial folds are observed


**FIGURE 2** Patient 62 y.o. before (A) and 3 mo after treatment (B). Improvement in facial color, skin tone, shallower wrinkles, pronounced lifting effect in the middle and lower thirds of the face, including shallower nasolabial and edge-labial folds is observed

| Measurement | Baseline (mm) | 30 d (mm) | 90 d (mm) |
|---|---|---|---|
| Epidermis thickness (mm) | 132. 21 ± 22.9 | 138.41 ± 24.06 | 134.87 ± 15.17* |
| Dermis thickness (mm) | 1324.62 ± 291.48 | 1422.09 ± 290.91 | 1489.58 ± 278.55* |
| Dermis density | 12.64 ± 4.5 | 13.45 ± 4.5 | 16.08 ± 4.34* |
| Hypodermis thickness (mm) | 434.81 ± 136.22 | 434.75 ± 153.82 | 448.38 ± 122.00 |
| SMAS thickness (mm) | 180.38 ± 63.55 | 209.1 ± 68.05* | 239.87 ± 65.11* |
| SMAS density | 18.93 ± 10.31 | 20.84 ± 10.34 | 27.39 ± 7.83* |

*Note:* Asterisk shows statistical significance ($P < .05$).

**TABLE 1** The clinical outcomes (mean value ± SD) of ultrasound skin examination at the baseline, 30 d and 90 d after the laser therapy

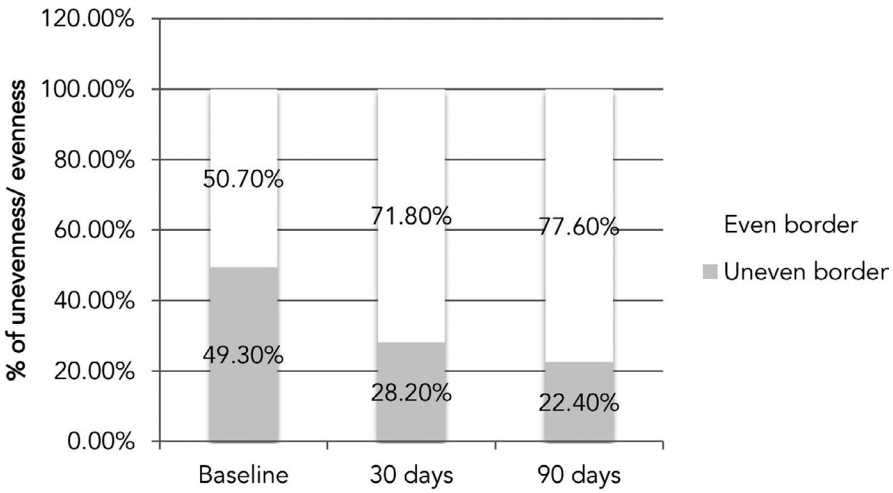


**FIGURE 3** The dermal-hypodermal boundary structure at baseline, 30 d and 90 d after laser therapy

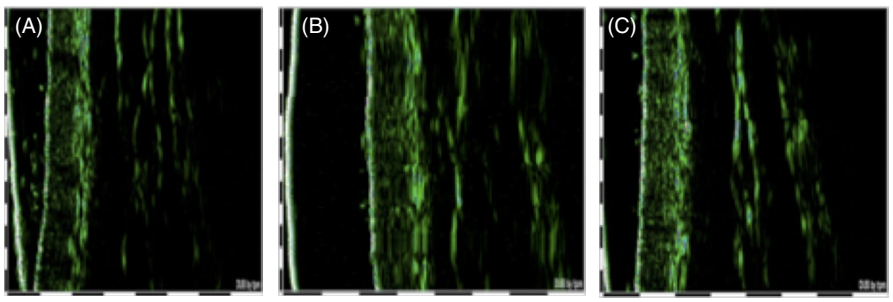


**FIGURE 4** Patient 50 y.o. Results of US scanning of soft facial tissues before (A), 30 d (B) and 90 d after treatment (C). Increase in the echogenic density of the dermis, mainly in the reticular layer and thickness and echogenic density, visualization over a longer portion of SMAS is shown (B, C)

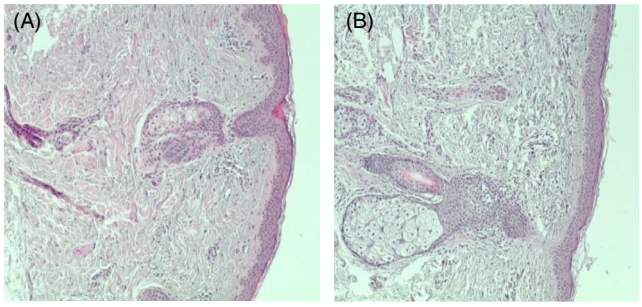


**FIGURE 5** Patient 46 y.o. Hematoxylin and eosin staining. Zoom ×100. (A) Before and (B) At 90 d after the treatment. An increase of epidermal thickness is observed

breakdown and elastosis. The collagen fibers were also fragmented, disoriented, with random scattered fragments not accompanied with elastic fibers (Figure 6A). At the 90-day follow-up, new collagen and elastin fibers, longitudinally oriented were observed in the papillary dermis (Figure 6B). Immunophenotyping of collagen revealed that at baseline type I, type III, and type IV collagen was decreased in the dermis and appeared in the form of disoriented thick short fragments (Figure 7-9A, 7-9A and 7-9A). At the 90-day follow-up, collagen type I was shown to be longitudinally oriented in fine fibrous structures, creating a collagenous framework of the papillary layer (Figure 7B), while in the reticular layer, type III collagen prevailed, with its bulk density slightly increased compared to baseline (Figure 8B). Finally, the amount of type IV collagen, which is the main type of collagen of the basal membrane of the epidermis, was shown to be significantly increased at the 90-day follow-up (Figure 9B).

## 4 | DISCUSSION

In this follow-up prospective clinical study, the objective was to thoroughly evaluate the biological effects of the recoSMA technology on

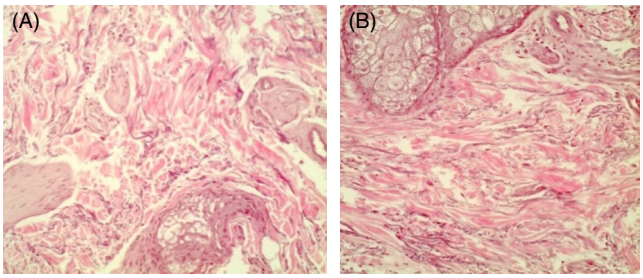


**FIGURE 6** Patient 46 y.o. Weigert's staining. Zoom ×200. (A) Before the treatment (B) At 90 d after the treatment. Collagen fibers form longitudinally oriented fine fibrous structures which are accompanied with elastic fibers

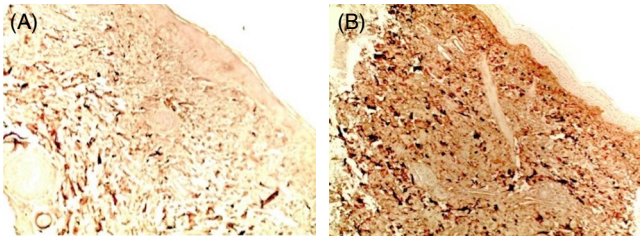


**FIGURE 7** Patient 52 y.o. Immunohistochemical examination. Collagen type I (Immunoperoxidase method, Rabbit Polyclonal). Zoom ×100. (A) Before the treatment (B) At 90 d after the treatment. Content of collagen type I in dermis is notably increased and longitudinally oriented collagen fibers are formed

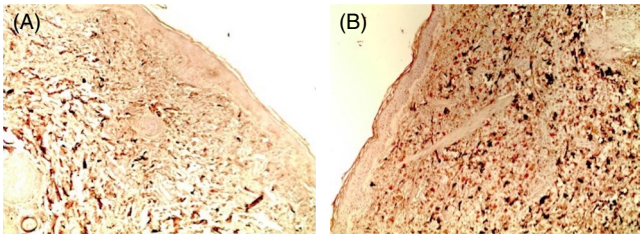


**FIGURE 8** Patient 52 y.o. Immunohistochemical examination. Collagen type III (Immunoperoxidase method, Rabbit Polyclonal). Zoom ×100. (A) Before the treatment (B) At 90 d after the treatment. Content of collagen type III in dermis is increased

the skin structures (dermis, epidermis) and the SMAS. Using ultrasound analysis, a significant increase of the dermal and SMAS thickness and density was shown at the 90-day posttreatment follow-up. Aside from the increase in thickness and density, the architectural framework of each layer was shown to be restored, with boundaries between the skin layers distinctly appearing after 90 days. The SMAS layer was also shown to regain its cohesivity, indicative of structural repair.

Aside from the ultrasound analysis, immunohistochemical studies showed pronounced changes in the epidermis and dermis. Correlating with the ultrasound data, there was a demonstrated increase of the epidermal thickness and an improvement of the epidermal basal membrane. Immunophenotyping of the collagen types, corroborated the increase in skin layer thickness with an increase level of collagen type I, III, and IV. The newly synthesized collagen fibers were found to be oriented longitudinally, restoring

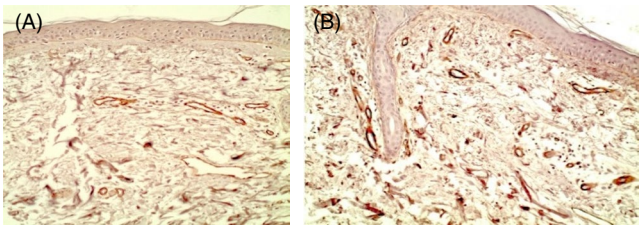


**FIGURE 9** Patient 46 y.o. Immunohistochemical examination. Collagen type IV (Immunoperoxidase method, CIV22). Zoom ×200. (A) Before the treatment (B) At 90 d after the treatment. Content of collagen type IV in the basal membrane and dermis is increased

the normal tissue pattern, with no evidence of fibrotic processes taking place.

The findings from the ultrasound and histological analysis, parallel the timing and intensity of clinical improvement observed in patients, with a gradual increase of facial rejuvenation at 30 days that peaks at the 90 days posttreatment follow-up.

Limitations of the study include the short follow-up time (90 days posttreatment) which coincides with the time of maximal improvement. Clinical studies using more long-term follow-up times to determine the durability of the clinical effect are currently in progress.

Collectively, this study confirms the results of an earlier study showing the clinical efficacy and safety of recoSMA treatment for facial rejuvenation, and in addition illustrates the recoSMA mechanism of action, which is based on induction of neocollagenesis and matrix remodeling.

## ORCID

*Neil S. Sadick* https://orcid.org/0000-0002-9542-4097

## REFERENCES

1. Sadick NS. Volumetric structural rejuvenation for the male face. *Dermatol Clin*. 2018;36(1):43-48.
2. Sadick NS, Dorizas AS, Krueger N, Nassar AH. The facial adipose system: its role in facial aging and approaches to volume restoration. *Dermatol Surg*. 2015;41(Suppl 1):S333-339.
3. Broughton M, Fyfe GM. The superficial musculoapouneurotic system of the face: a model explored. *Anat Res Int*. 2013;2013:794682.
4. Brun C, Jean-Louis F, Oddos T, Bagot M, Bensussan A, Michel L. Phenotypic and functional changes in dermal primary fibroblasts isolated from intrinsically aged human skin. *Exp Dermatol*. 2016;25(2):113-119.
5. Francu LL, Hinganu D, Hinganu MV. Anatomical evidence regarding the existence of sustentaculum facies. *Rom J Morphol Embryol*. 2013;54(3 Suppl):757-761.
6. Britt CJ, Marcus B. Energy-based facial rejuvenation: advances in diagnosis and treatment. *JAMA Facial Plast Surg*. 2017;19(1):64-71.
7. Zachary CB. Facial rejuvenation: 40th anniversary review. *Semin Cutan Med Surg*. 2016;35(6 Suppl):S122-124.
8. Sadick NS. Antiaging and whole-body rejuvenation. *J Drugs Dermatol*. 2008;7(4):329.
9. Volkova NV, Glazkova LK, Khomchenko VV, Sadick NS. Novel method for facial rejuvenation using Er:YAG laser equipped with a

spatially modulated ablation module: an open prospective uncontrolled cohort study. *J Cosmet Laser Ther*. 2017;19(1):25-29.
10. Hersant B, SidAhmed-Mezi M, Chossat A, Meningaud JP. Multifractional microablative laser combined with spacially modulated ablative (SMA) technology for facial skin rejuvenation. *Lasers Surg Med*. 2017;49(1):78-83.
11. Pikirenia I, Khomchenko VV. Possibilities of liver regeneration with induced cirrhosis at exposure of spatially modulated erbium laser radiation in experimental animals. *Surg News*. 2015;23(2):131-137.
12. Trelles MA, Khomchenko V, Alcolea JM, Martinez-Carpio PA. A novel method of facial rejuvenation using a 2940-nm erbium:YAG laser with spatially modulated ablation: a pilot study. *Lasers Med Sci*. 2016;31(7):1465-1471.
13. Meningaud JP, SidAhmed-Mezi M, Billon R, Rem K, La Padula S, Hersant B. Clinical benefit of using a multifractional Er:YAG laser combined with a spatially modulated ablative (SMA) module for the treatment of striae distensae: a prospective pilot study in 20 patients. *Lasers Surg Med*. 2019;51(3):230-238.

**How to cite this article:** Volkova NV, Valamina IE, Shvidun DV, Rebrieva AS, Sadick NS. Facial rejuvenation using Er:YAG laser equipped with a spatially modulated ablation module: A clinical, ultrasound, and histological evaluation. *J Cosmet Dermatol*. 2019;00:1–6. https://doi.org/10.1111/jocd.13083